Thermo-mechanical performance of a proposed energy pile system in cold regions

Maryam Saaly[a], Pooneh Maghoul[a], Hartmut Hollaender[a], Ali Fatolahzadeh[a]

[a] *Department of Civil Engineering, University of Manitoba, 15 Gillson St., Winnipeg, MB, Canada, R3T 5V6*

Abstract

Energy piles are bi-functional structural elements that are used to support the structural loads of a building and to operate as a geo-heat exchanger for shallow geothermal energy systems. In urban areas, energy piles can eventually be used to harvest the heat loss through the basement enclosure and re-inject the energy to the building for the heating and cooling purposes. In spite of a higher thermal profile beneath the buildings due to energy loss through the below-grade envelope, an underground thermal imbalance may still occur due to the application of energy piles in cold regions. This paper aims to study the structural performance of an energy pile in cold regions considering the potential occurrence of thermal imbalance in the foundation soil through a Thermo-Mechanical (TM) analysis. This will be the first step of adoption of such a technology in Canadian cold climate. Results showed a safe margin between the pile settlement and the allowable settlement. However, the axial stress applied to the pile increased by 9% due to thermal loads. In addition, a maximum decrease of 9% in mobilized shaft friction along the pile-soil interface was recorded due to the thermal loads. To consider the energy piles as an alternative for buildings energy supply in cold regions, further considerations should be made to keep the mechanical response of the energy piles in the admissible range.

Keywords: Geothermal pile, Thermal imbalance, Geothermal energy, TM model, cold regions

1. Introduction

The energy consumption has increased all over the world due to the population growth and industrial needs. One of the alternatives to address this increasing energy demand is the application of new technologies to harness the energy stored in the ground due to the moderate temperature of the ground all over the year [1, 2]. One of the most promising technologies for the application of geothermal energy is the Ground Source Heat Pump (GSHP). Such a system consists of a heat pump, ground heat exchangers, and a heat distribution system. The ground heat exchangers (GHEs) can be an open-loop or a closed-loop system and its selection depends on various parameters that impact the feasibility of the project

*Corresponding author

Email address: Pooneh.Maghoul@umanitoba.ca (Pooneh Maghoul)

such as the availability of natural groundwater, ponds or lakes. Despite the simple design and better thermodynamic performance of an open-loop system, environmental regulations restrict the application of this type of GHE. In fact, changes in groundwater temperature during the operation of GSHP may result in an increase in the bacterial content and suspended particles in groundwater [3].

On the other hand, closed-loop systems can be installed horizontally (straightly horizontal or spirally horizontal loops placed in trenches) or vertically (U-shaped, W-shaped or spiral loops placed in boreholes) depending on the availability of land and energy demand. One of the disadvantages of the application of horizontal loops in cold regions like Canada is that the ground temperature is subjected to seasonal variation at shallow depths [4]. However, the installation costs of vertical closed-loop systems can be fairly highly dependent on depth and the required number of boreholes [5]. To overcome this issue, a rapidly growing construction technology, which integrates the geothermal energy technique into the structural pile foundation system has been developed [6–9]. The geothermal pile operation principle is based on the circulation of a heat carrier fluid in polyethylene pipes embedded in the piles through which heat exchange occurs between the energy pile and the surrounding medium [10–13]. This energy further feeds the GSHP system so that the energy pile acts as heat exchangers in addition to their main function as structural support elements.

Geothermal piles are broadly applied in European countries [9, 14–18]. For example, Bourne-Webb et al. [14] conducted some in-situ tests on a single energy pile installed in London Clay. The main scope of the in-situ tests was to evaluate the mechanical performance of the pile subjected to thermal cycles. The temperature and strain profiles of the tested pile were recorded using an optical sensor system, vibrating-wire strain gauges, thermistors, and external load control elements. Based on the obtained results, variations in the temperature of the pile, depending on whether the pile is heated or cooled, changed the mobilized shaft friction along the pile-soil interface. It was speculated that if the margin between the pile ultimate shaft resistance and shaft friction along the soil-pile interface is large enough, the pile capacity will not change significantly.

Although full-scale in-situ experiments are more reliable to evaluate the TM response of energy piles, they usually require a fair amount of budget and time. An alternative approach to estimate the behavior of the energy piles is analytical or numerical studies. For example, Pasten and Santamarina [19] evaluated the mechanical behavior of energy piles using the one-dimensional load transfer method. This study emphasized on the importance of the first few cycles of thermal loading in assessing the pile head displacement and corresponding shaft friction variations.

Jeong et al. [20] carried out a three-dimensional (3D) finite element analysis to quantify the axial load and settlement of energy piles in a group which are subjected to TM loading. This study highlighted the importance of soil type on the mechanical response of the energy piles. It was concluded that the head displacement of the energy piles embedded in clay was up to 1.5 mm larger than the head displacement of piles installed in sand although both cases were in acceptable limits.

One of the significant advantages of numerical analysis over in-situ tests is the potential for studying the behavior of energy piles over long-term periods. Olgun et al. [21] studied the long-term displacement of different arrangements of energy piles over a 30-year span of time under different climatic conditions. Impact of climate condition manifested itself as a variation in the ground temperature as well as a variation of energy demand of the building for which the energy foundation was designed. This factor has been studied by Saaly et al. [22] Liu et al. [23], Dacquaya et al. [24], and Andolfi et al. [16].

Although broadly expanded in Europe and the USA, in Canada, the application of geothermal piles is not well established and limited knowledge regarding the thermal and mechanical operation of such systems exists. In Canada, the operation of GSHP systems may not be satisfactory and may degrade over a few years of the operation of energy piles [25]. The reason for such malfunction is underground thermal imbalance, which is the term used for the gradual decrease in the ground temperature over years because of an excessive heat extraction for heating the space during the long winter season. As soil temperature decreases, the outlet temperature of the GHE lowers gradually. This contributes to the deterioration of the heating performance of the GSHP. In addition, the underground thermal imbalance and excessive heat extraction can decrease the soil temperature below the freezing point. This causes freezing at the pile-soil interface which temporarily increases the bearing capacity of the energy pile. However, during spring, thawing occurs at the soil-pile interface, which decreases the bearing capacity of the piles significantly. The occurrence of such freezing and thawing cycles at the soil-pile interface adversely affects the structural integrity as well as the energy efficiency of such systems [26]. Therefore, it is of paramount importance to consider the potential occurrence of ground thermal imbalance, i.e. the energy performance, in the design of geothermal pile foundation systems in cold regions.

In urban areas, the ground temperature below the buildings base area is fairly higher in comparison to open fields due to the heat dissipation of buildings through their sub-grade enclosures [27]. For example, Saaly et al. [28] showed that for an institutional building in the campus of the University of Manitoba with approximate annual heat loss of 30 MWh through the below-grade envelope, soil temperature could increase up to 5°C comparing to the situation that no heat loss occurs through the building's basement. Such heat source can only be targeted by energy piles since the hot spot of each heat loss is beneath the building. Therefore, the lost energy can be re-harvested using a geothermal foundation system which favorably affects the efficiency of the GSHPs. Moreover, this additional dissipated heat from the building basement can ameliorate the potential thermal imbalance in the ground. In this regard, Saaly et al. [22] conducted a study to determine the thermal capacity of a proposed hypothetical geothermal foundation system considering the heat loss through the basement of an institutional building in cold regions. The energy piles are subjected to both thermal loads due to temperature variations of the fluid heat exchanger whose magnitude is a function of the building heating and cooling demand as well as structural loads [29]. Therefore, aside from the energy performance of the system, the impacts of thermal loading on the structural performance of geothermal piles should be assessed. For example, thermal loads cause volumetric expansion and contraction when piles are heated and cooled, respectively. In addition, the thermo-mechanical properties of soils surrounding the pile foundation are temperature-dependent, which can affect the interaction between the soil and foundation at their interface [30].

Although above-mentioned numerical works proposed the geothermal system for re-harvest of buildings energy loss, mechanical response of the proposed energy piles used in buildings foundation yet needs to be investigated. Therefore, this paper aims to investigate the thermo-mechanical behavior of a single pile in an energy foundation system, which is designed for energy supply of an institutional building in Winnipeg, Canada. This foundation system is subjected to heat dissipation through the below-grade enclosure of the building. The present work is intended to provide a tool for prediction of the thermo-mechanical response of energy piles by incorporating the knowledge of buildings energy loss.

2. Features of the Energy Foundation System

The energy foundation system belongs to a four story institutional building, the Stanley Pauley Engineering Building (SPEB), with a total base area of 1,150 m^2 located in Winnipeg (MB), Canada. Winnipeg experiences an average daily temperature fluctuation that ranges from +20°C in summer to -20°C in winter [31]. Consequently, the buildings in Winnipeg usually have a high energy demand, both for heating and cooling purposes [32].

Winnipeg soil is mainly composed of fine-grained deposits of Lake Agassiz that are followed by Precambrian basement of bedrock [27]. Based on the site investigation reports, the stratigraphy of the site consists of a layer of dark grey clay deposits having a thickness of 2 m overlaying a 14.7 m thick layer of brown clay followed by a dense layer of till deposits [33].

The foundation of the building consists of 119 concrete micro-piles designed for an ultimate limit state axial resistance of 1000 kN, which are embedded at the depth of -4.25 m below grade. Saaly et al. [22] proposed a geothermal foundation system in which all the 119 piles were considered to be energy piles and were equipped with heat carrier pipes. In other words, all piles are assumed to operate as a geothermal heat exchanger to supply the SBEB energy demand (Fig. 1). To this end, the foundation piles are equipped with heat carrier pipes to exchange heat with the surrounding medium.

To determine the inlet temperature of fluid in the heat

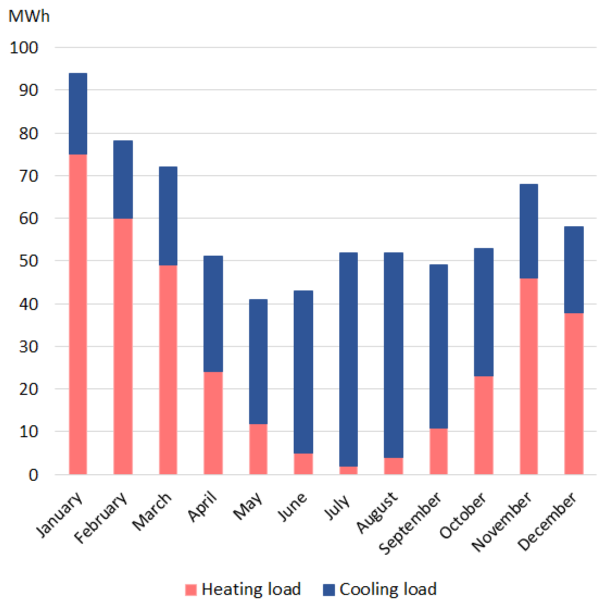

Figure 1: Monthly heating and cooling energy demand of the Stanley Pauley Engineering Building [32].

exchanger pipe, two main factors have been considered: (i) meeting the thermal balance of the ground during the heat extraction and rejection, (ii) avoiding freezing at the soil-pile interface. Considering the mentioned criteria, the flow rate of the heat exchanger fluid entering the closed loop embedded in the pile is chosen as 30.5mo lit/min while its inlet temperature varies between -1°C during Nov–Apr and 20°C during May–Oct. Based on the results, up to 41% of the energy demand of the Stanley Pauly building can be supplied using an energy pile foundation system by meeting the ground thermal balance and avoiding the freezing at the soil-pile interface [22]. Knowing the inlet temperature of the heat exchanger fluid, the mechanical behavior of a single geothermal pile in the foundation system of the SPEB is evaluated in the following sections.

3. Thermo-Mechanical Model

3.1. Governing Equations

A coupled thermo-mechanical model has been applied to assess the mechanical and thermal behaviors of one of the piles of the SPEB foundation equipped with a heat exchanger pipe. The governing equations applied to study the thermo-mechanical behavior of the geothermal pile in contact with the surrounding soils are based on the following assumptions:

- Soil is considered to be fully-saturated having two-phases (solid skeleton and water). The soil is modeled as an isotropic, elastoplastic material. The Mohr-Coulomb constitutive model is used to determine the size of the yield surface in the soil.
- Pile material is taken to be solid, isotropic and linear elastic.
- Perfect contact has been assumed at the interface between the soil and pile.
- The solid grains and fluid phase of the soil are modeled as incompressible materials.

To consider the equilibrium of forces in the domain, the conservation of linear momentum in absence of inertial terms is applied:

$$\nabla.\sigma + \mathbf{b} = 0 \quad (1)$$

where $\nabla.$ is the divergence operator, σ is the total (Cauchy) stress tensor and $\mathbf{b}$ is the body force vector which can be determined as shown below:

$$\mathbf{b} = \rho\, \mathbf{g} \quad (2)$$

where, $\mathbf{g}$ is the gravitational acceleration vector and ρ is the average bulk density of the soil which can be determined by the following equation:

$$\rho = (1-n)\, \rho_s + n\, \rho_w \quad (3)$$

in which ρ_s and ρ_w are the density of solid skeleton and water, respectively. n is the porosity of the soil.

The constitutive law of the solid skeleton describing the stress-strain relations is defined in terms of the effective stress as described in Eq. 4.

$$\boldsymbol{\sigma'} = \boldsymbol{D^e}\, (\boldsymbol{\varepsilon} - \boldsymbol{\varepsilon^T} - \boldsymbol{\varepsilon_{pl}}) \quad (4)$$

where $\boldsymbol{D^e}$ is the elastic stiffness tensor, $\boldsymbol{\varepsilon}$ is the strain tensor, $\boldsymbol{\varepsilon^T}$ is the thermal strain tensor, and $\boldsymbol{\varepsilon_{pl}}$ is the plastic strain tensor. Plastic strains are computed by the Mohr-Coulomb yield criterion. Also, the thermal strains are computed using the following equation:

$$\boldsymbol{\varepsilon^T} = \frac{1}{3}\, (\alpha_s \nabla T)\, \boldsymbol{I} \quad (5)$$

in which $\boldsymbol{\varepsilon^T}$ is the thermal strain tensor, $\boldsymbol{I}$ is the second order unit tensor, α_s is the volumetric thermal expansion coefficient, ∇ is the gradient operator, and T stands for the temperature.

To determine the heat transfer in porous media, the energy conservation equation is described below:

$$\rho C\, \frac{\partial T}{\partial t} + \nabla.\, q_c = 0 \quad (6)$$

where ρC is the volumetric heat capacity of the soil which is a function of volumetric heat capacity of solid skeleton ($\rho_s C_s$) and pore water ($\rho_w C_w$) as described below:

$$\rho C = (1-n)\, \rho_s C_s + n\, \rho_w C_w \quad (7)$$

In Eq.7, q_c [W/m^2] is the conductive heat flux through the volume which is defined by Fourier's law as follows:

$$q_c = -\lambda\, \nabla T \quad (8)$$

where λ denotes the effective thermal conductivity of the material whose value for the soil can be determined as described in Eq. 9.

$$\lambda = (1-n)\, \lambda_s + n\, \lambda_w \quad (9)$$

in which λ is the effective thermal conductivity of the soil, λ_s is thermal conductivity of solid grains and λ_w is thermal conductivity of water.

3.2. Numerical Model

The numerical model has been implemented in the finite-element commercial software COMSOL Multiphysics. The dimension of the 2D axisymmetric model applied in this study is 10 m × 10 m. On top of the soil domain, a 0.23 m thick layer of thermal insulation and a 0.2 m thick layer of concrete slab are placed (Fig. 2). The modeled pile is a friction pile which has a diameter of 0.4 m and a length of 5 m. The thermo-mechanical properties of the materials used in the model (soil (in wet condition), concrete and insulation) are summarized in Table 1.

Based on the structural and design documents, 5 m micro-piles have been used in the foundation of the SPEB considering the structural load and geotechnical parameters.

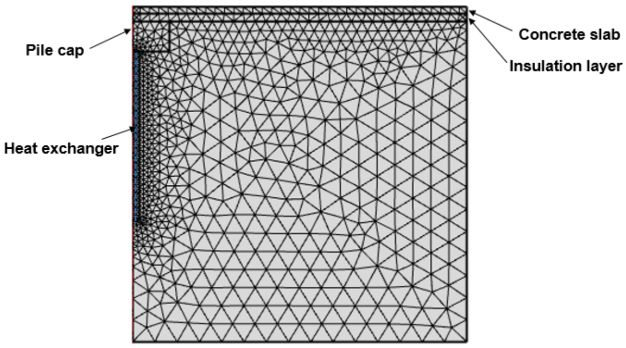

Figure 2: Axisymmetric finite elements model.

The boundary conditions of the thermo-mechanical (TM) model are as follows:

- The thermal boundary conditions: Constant temperature on the heat exchanger, adiabatic condition at the bottom and surrounding boundaries are considered. Also, to estimate the impacts of heat dissipation through the building basement slab, a convective heat flux q_0 $[W/m^2]$ is assigned to the top boundary of the model as follows:

$$q_0 = h\,(T_{indoor} - T_s) \tag{10}$$

where h is the convective heat transfer coefficient whose value is assumed to be equal to 6 W/m^2°C [26], T_{indoor} is the basement indoor air temperature that is assumed constant and equal to 20°C, T_s [°C] is the temperature at the ground surface.

- The mechanical boundary conditions: The roller condition on the right boundary of the model, and fixed constraint at the bottom of the domain are considered. An axisymmetric condition is assumed from the left boundary.

Soil	
Young's modulus [Pa]	70×10^6
Poisson ratio [-]	0.236
Density [kg/m^3]	1767
Thermal conductivity [W/m°C]	1.483
Specific heat capacity [J/kg°C]	960
Thermal expansion coefficient [1/K]	1.7×10^{-5}
Porosity [-]	0.535
Cohesion [kPa]	5
Friction angle [°]	18

Concrete	
Young's modulus [Pa]	40×10^9
Poisson ratio [-]	0.2
Density [kg/m^3]	2300
Thermal conductivity [W/m°C]	1.5
Specific heat capacity [J/kg°C]	880
Thermal expansion coefficient [1/K]	8.5×10^{-6}

Insulation	
Density [kg/m^3]	34
Thermal conductivity [W/m°C]	0.041
Specific heat capacity [J/kg°C]	1450

Table 1: Properties of SPEB's numerical model.

The initial temperature of the model is assumed to be equal to 8°C [22]. Also, the initial stress conditions are obtained from the results of another steady-state simulation considering only the gravity effects. In other words, the finite element analysis has been done in two stages. Through the first stage, a steady state analysis has been carried out while considering the gravity effects to gen-

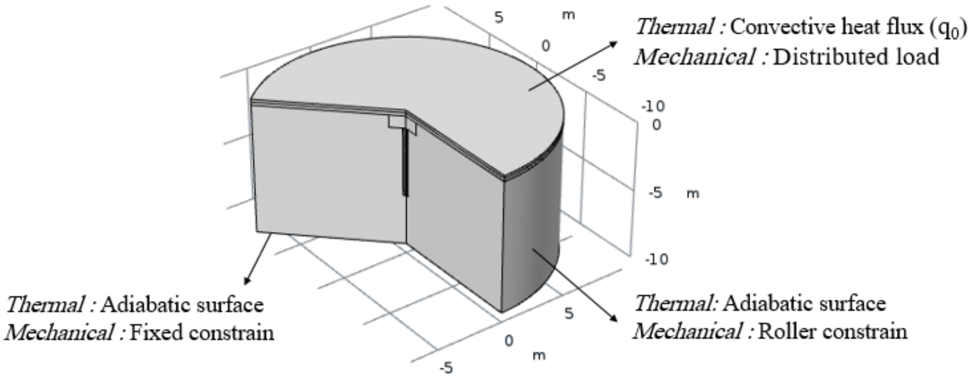

Figure 3: The thermo-mechanical boundary conditions applied to the model.

erate the initial stresses as the input for the transient simulation. In the transient stage, the energy pile response to the applied axial load and thermal cycles has been studied over a five-year span of time.

3.3. Model Validation

To validate the implemented TM model in this work, experimental data studied by Bourne-Webb et al. [14] has been used. The experimental data obtained from the full-scale study that was undertaken on a test pile that was equipped with the heat exchanger pipes. The mentioned pile was designed as part of a 143 piles foundation system of a five-storey building that was located in the Clapham Centre of Lambeth College London and functioned as a geothermal heat exhchanger of a GSHP system. The pile is installed in the London clay whose properties are reported in Table 2.

The conducted tests included both heating and cooling cycles in conjunction with a mechanical load. The test pile response to the applied thermo-mechanical loads was obtained using Vibrating Wire Strain Gages (VWSG) and Optical Fibre Sensors (OFS). As shown in Fig. 4, the first stage of the experiment included applying a 1200 kN mechanical load. During the cooling stage, a thermal load of ΔT = -19°C in addition to the 1200 kN mechanical load was applied to the pile. Finally, the heating phase which consisted of the mechanical load and a thermal variation of ΔT = +10°C was carried out.

Property	Concrete	London Clay
Young's modulus [Pa]	40×10^9	70×10^6
Poisson ratio [-]	0.2	0.236
Unit weight [kN/m^3]	20	20
Thermal conductivity [W/m°C]	2.33	1.79
Specific heat capacity [J/kg°C]	960	910
Thermal expansion coefficient [1/K]	8.5×10^{-6}	4×10^{-5}
Hydraulic conductivity [m/s]	-	1×10^{-11}
Porosity [-]	-	0.4

Table 2: Characteristics of the validation model's material

The initial temperature of the pile and soil in the London case had been assumed constant over the entire domain and equal to 19.5°C and the thermo-mechanical loading time applied in this study lasted for almost 1250 days.

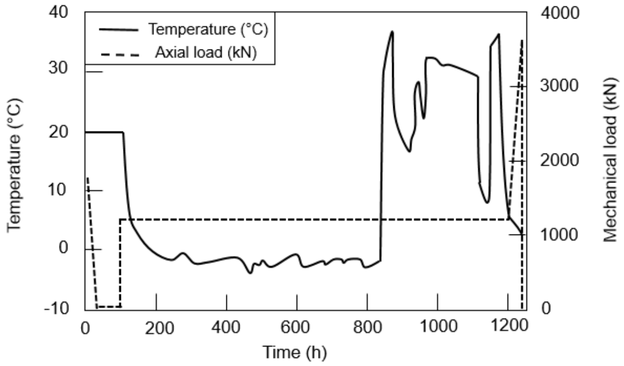

Figure 4: Thermo-mechanical loading history of experimental case (Bourne-Webb et al. [14])

Comparing the pile head displacements obtained from the experimental tests and the numerical model, good agreement was found during the cooling phase (100 – 860 h) (Fig. 5). Although the magnitude of vertical displacement of the pile head during the heating loading is slightly lower in the numerical model, the similarities are acceptable from an engineering point of view to consider the model an appropriate tool for predicting the thermo-mechanical behavior of the energy pile.

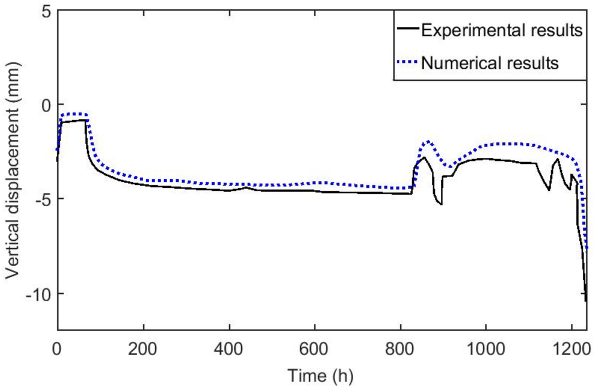

Figure 5: Comparison between the numerical and field data regarding the vertical displacement of the pile head.

Fig. 6 and Fig. 7 provide a comparison between the experimental data which were obtained from two measurement systems (VWSG and OFS) and the numerical results in terms of mobilized shaft friction along the pile-soil interface and axial load along the pile axis. A two-tailed student's t-test is carried out with 95% level of confidence in which a null hypothesis "Any differences, discrepancies, or suspiciously outlying results are purely due to random and not systematic errors" is made. The p-value which is an outcome of the t-test shows the acceptance or rejection of the null hypothesis. For correlation between the numerical and the experimental results with 95% level of confidence, p-value > 0.05 is required for every set of data. The obtained p-value for each of the validation graphs are provided in Table 3. The numerical results that were obtained from the TM model showed a good agreement with the experimental data reported by Bourne-Webb et al. [14].

3.4. Thermo-Mechanical Loading History of the Energy Pile in SPEB

The validated numerical model in COMSOL Multiphysics is applied to investigate the behavior of one of the geothermal piles of the SPEB's foundation. The total loading time was 1825 days (five years) which included the seasonally cyclic thermal loads (i.e., 6 months heating and 6 month cooling per year) in addition to a constant mechanical load. The mechanical load was equal to the ultimate capacity of the friction pile (i.e. 1000 kN) that is applied with a factor of safety of 3. It should be noted that the bearing capacity of the

p-value	mobilized shaft friction (VWSG)	mobilized shaft friction (OFS)	Axial load (VWSG)	Axial load (OFS)	Pile head displacement
Mechanical loading	0.134	0.509	0.134	0.101	
Heating loading	0.845	0.447	0.572	0.160	0.061
cooling loading	0.837	0.441	0.100	0.577	

Table 3: Summary of the p-values obtained from the student's t-test.

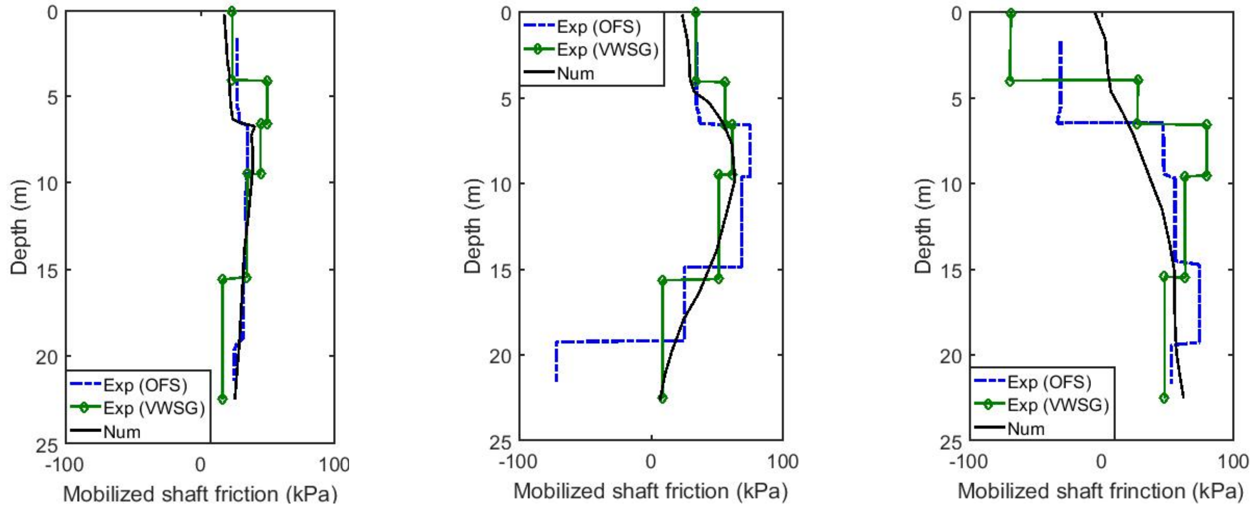

(a) Mechanical load (b) Mechanical + Cooling load (c) Mechanical + Heating load

Figure 6: Comparison between numerical (Num) and experimental (Exp) results of mobilized shaft friction along the pile-soil interface.

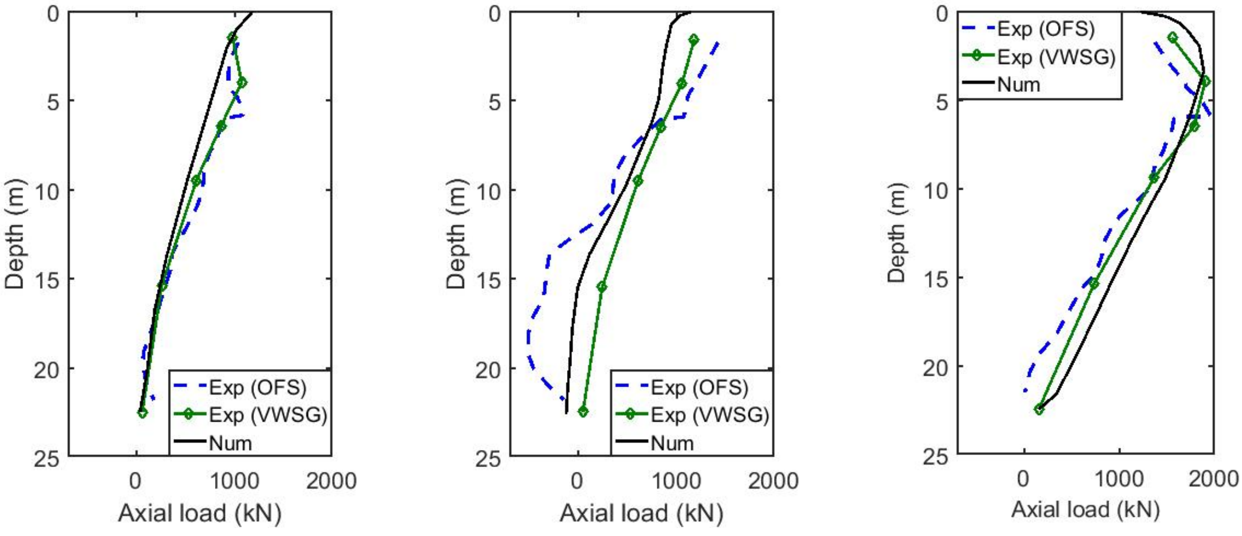

(a) Mechanical load (b) Mechanical + Cooling load (c) Mechanical + Heating load

Figure 7: Comparison between numerical (Num) and experimental (Exp) results of axial load along the length of the pile.

pile is computed by the ultimate end-bearing, and ultimate skin friction capacities.

As mentioned earlier, the thermal load is applied to the pile while the heat transfer fluid circulates in the heat exchanger pipes. In this work, such a thermal load is represented by a constant temperature, which is equal to the inlet temperature of the heat exchanger fluid, along the length of the heat exchanger pipe. Based on the numerical study carried out by Saaly et al. [22], the inlet temperatures of the pipe have been suggested to be equal to 20°C during May–Oct, and -1°C during the 6 cold months (Nov-Apr) of the year. As mentioned before, the inlet temperatures were chosen to meet the thermal balance of the ground during heat extraction and rejection over the year as well as to avoid freezing at the soil-pile interface. Fig. 8 provides the seasonal variation of the inlet temperature of the heat exchanger probes as well as the mechanical load applied to the head of the pile.

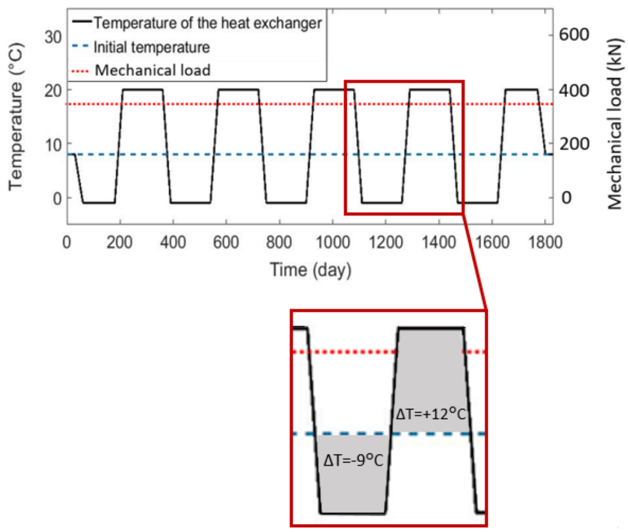

Figure 8: Time histories of applied thermal and mechanical loads.

To demonstrate the initial pile settlement due to only the mechanical load, during the first 30 days of the simulation the temperature in the probes are equal to the initial temperature ($T_{initial}$ = 8°C). In addition, during the last 30 days of the loading time history, the temperature of the probes are equal to 8°C to evaluate the reversibility of pile head displacement induced by the thermal loads.

4. Results and Discussion

To study the performance of an energy pile subjected to thermo-mechanical loadings, the vertical displacement of the pile, the maximum axial load induced by the thermo-mechanical loads and the mobilized shaft friction along the pile-soil interface are investigated in this section. The reason is that such factors are considered in the Limit State-based geotechnical design.

The energy pile and its surrounding soils were subjected to an additional thermal load due to the heat loss through the slab of the basement floor. Such heat dissipation from the basement into the ground occurred in spite of insulating the basement envelope [34–37]. The reason was that the basement slab was in direct contact with the foundation soil whose temperature was different from the regulated temperature of the basement indoor air. Consequently, the thermal gradient between the foundation soil and basement indoor air contributed to heat loss via the thermal conduction through the floor slab [22, 38]. The impacts of such heat leakage is often ignored while assessing the energy piles behavior. Therefore, this heat loss was incorporated in the model using a convective heat flux which was assigned to the basement slab surface. The energy pile response to the thermo-mechanical loading is provided for two cases: without considering heat loss through the basement slab

(Case 1) and with considering the basement energy loss (Case 2).

4.1. *Pile Head Displacements*

The initial pile head displacement that was induced by the mechanical load at the end of the first 30 days of the simulation time history was equal to -0.79 mm (Fig. 9). Once heat extraction from the ground by applying a $\Delta T = -9^{\circ}$C began, further pile head displacement occurred whose maximum reached to -1.19 mm at t = 182 days (i.e., the end of the heating season of the first year of the system operation). Such an observation was induced due to the contraction of the pile due to the temperature decrease in the probes with respect to the initial temperature of the pile (Fig. 8). For the case with no heat loss through the basement (Case 2), the minimum pile head displacement reached -1.18 mm at t = 182 days. This means that during the first few months of the analysis, the heat loss through the slab was not effective enough to influence the pile head displacement. This could be because of the significant thermal mass of the ground in the short time.

In contrast, during the heating loading (May–Oct), the geothermal pile expanded upon a +12°C temperature increase. The maximum expansion, whose value was +0.43 mm relative to the initial settlement, happened at t = 1795 days (i.e., the end of the cooling season of the fifth year of analysis). However, without considering the energy loss from the slab, the maximum expansion reached to +0.31 mm which showed occurrence of 15% less expansion compared to the maximum expansion of the pile head in Case 2. This discrepancy was due to heat leakage through the basement which increased the soil temperature near the basement floor and correspondingly caused more expansion at the pile head. It should be noted that the computed pile displacements (Fig. 9) were considerably less than the acceptable settlement (i.e., 25 mm) recommended by the National Building Code of Canada [39].

During the last 30 days of the operation of the system (i.e. at the end of the fifth year; 1795–1825 days), the inlet temperature of the pipes was set equal to the initial temperature of the pile ($T_{initial}$ = 8°C) to evaluate the reversibility of displacement induced by the thermal loads. It was observed that 40% and 25% of the initial pile head displacement left in the pile for the cases with and without considering heat loss, respectively. In other words, the vertical displacements of the pile head were not fully reversible which is suspected to be due to the elastoplastic behavior of the soil. In addition, for the case in which the basement energy loss was taken into account, the soil temperature increased up to 1.5°C near the basement floor. Therefore, a larger residual displacement was observed for this case.

4.2. *Axial Load and Mobilized Shaft Friction Variations*

In Case 1, in the stage in which the pile was subjected to only mechanical load, the pile was fully compressed. However, when a cooling load was applied in addition to the mechanical load to extract heat from the ground ($\Delta T < 0^{\circ}C$), the concrete pile contracted. Pile contraction induced tensile forces in the pile. Therefore, the

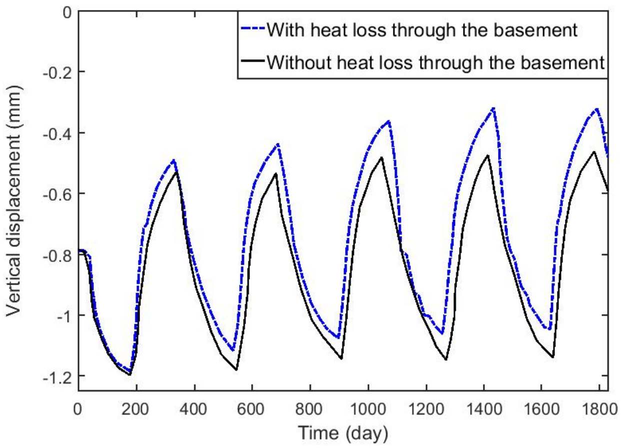

Figure 9: Vertical displacement of the pile head with and without consideration of the heat leakage from the SPEB basement.

axial load along the pile length decreased compared to the only mechanical loading stage. The maximum reduction in axial load that was applied on the pile due to the cooling load is 28 kPa (i.e., 9% reduction in the axial load during cooling stage loading compared to mechanical loading stage) that occurred at 0.9 m below the pile head (Fig.10a).

Contrary, at the end of the heating loading stage, compressive forces were generated in the pile due to the pile expansion. Consequently, up to 3% increase in compressive load compared to the initial mechanical load applied on the pile (i.e., 333 kN) was observed along the length of the pile.

According to the results regarding the axial load along the pile axis for Case 2, at the end of heating loading stage, the pile was up to 9% more compressed compared to the initial mechanical load applied on the pile (i.e., 333 kN) (Fig. 10b). It was observed that the maximum compressive load in Case 2, which was equal to 363 kN, was induced at the pile depth of 0.6 m during the heating loading stage. While the maximum axial load that was induced during heating loading at the same pile depth in Case 1 was 342 kN which was 6% lower than the maximum axial load in Case 2. The reason was the additional pile expansion in Case 2 due to the heat loss through the basement. Such results signify that considering the buildings heat leakage through the underground enclosure in urban areas may be an important factor in assessing the energy pile response to thermo-mechanical loading.

The axial load distribution illustrated in Fig. 10 signified that the thermal cycles change the magnitude of the induced axial load along the pile. In other words, the heating load (i.e., $\Delta T = +12^{\circ}$C) increased the induced axial load along the pile up to 9%. Such an increase in the axial load along the pile should be addressed in the geotechnical design by considering a higher factor of safety. For example, in Case 2 that the obtained maximum compressive axial load along the pile axis was 363 kN, 9% increase in the factor of safety (initially considered to be equal to 3.0) is required to ensure safe application of the energy pile since the pile was initially designed for allowable load of 333 kN. In practice, a factor of safety of at least 3.5 fulfils the required safety margin for the pile that is studied in this work.

The distribution of the mobilized shaft frictions along the pile-soil interface under three different conditions; (i) mechanical loading, (ii) heating and mechanical loadings, and (iii) cooling and mechanical loadings are provided in Fig. 11. During only the mechanical loading, the direction of the skin friction was upward and de-

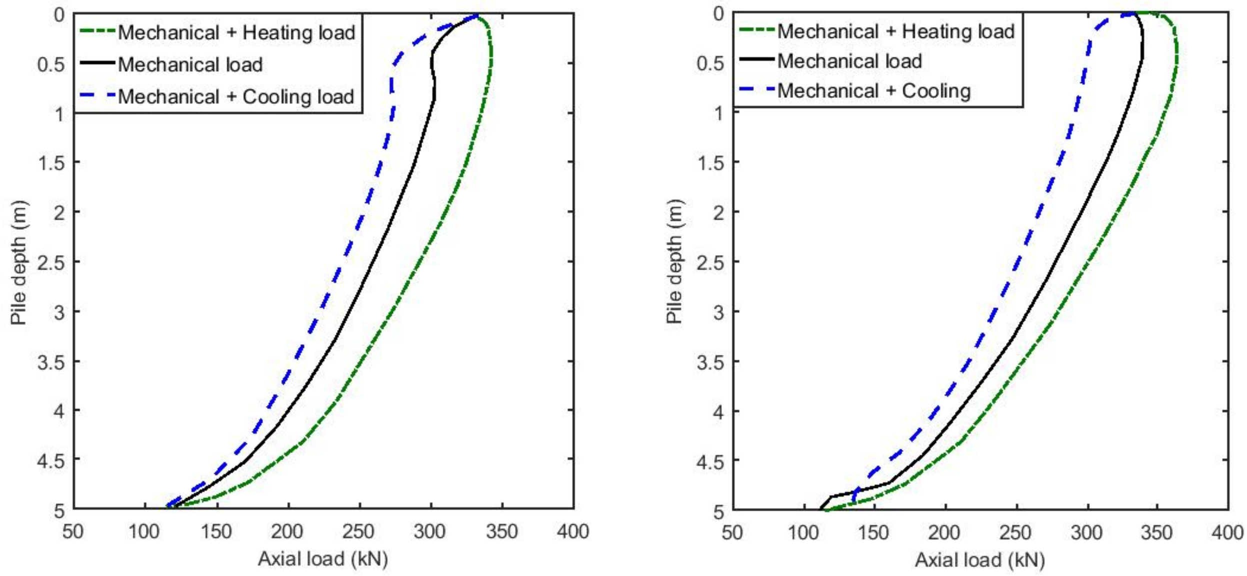

(a) Without considering the heat loss through the basement

(b) Considering the heat loss through the basement

Figure 10: Axial load distribution along the pile axis.

creased by depth. However, during the cooling loading stage (i.e., winter) the mobilized shaft friction along the length of the pile, upper than the neutral point, increased (maximum 3% increase in mobilized shaft friction at the pile depth of 0.3 m compared to the mechanical loading stage) while along the length of pile, lower than the neutral point, decreased up to 9% due to the contraction of the concrete pile. Conversely, during the heating loading stage that expansion occurred in the pile, the mobilized shaft friction increased up to 5% along the length of the pile lower than the neutral point while along the upper part of the pile it decreased (maximum 3% decrease in mobilized shaft friction at the pile depth of 0.2 m compared to the mechanical loading stage).

Comparing the mobilized shaft frictions resulted from Case 1 and Case 2, it is observed that in Case 2 in which heat loss through the basement added more heating load to the ground, shaft frictions decreased up to 4% compared to Case 1. This happened since the additional heating load especially close to the basement floor induced more expansion compared to Case 1. This expansion led to a downward pile-soil friction which contributed to a lower shaft friction along the pile-soil interface in Case 2 compared to Case 1.

4.3. Thermal field

The temperature profiles produced by the variation of the inlet temperature of the heat exchanger pipe in Case 1 are illustrated in Fig.12. The temperature fields of the model are provided for three stages of loading. In the first stage, the mechanical loading was only applied to the pile (Fig.12a). Since no thermal load was implemented in this stage, the temperature of the all domain was equal to the initial temperature ($T_{initial}$ = 8°C).

At the end of the cooling loading stage 12c, when the

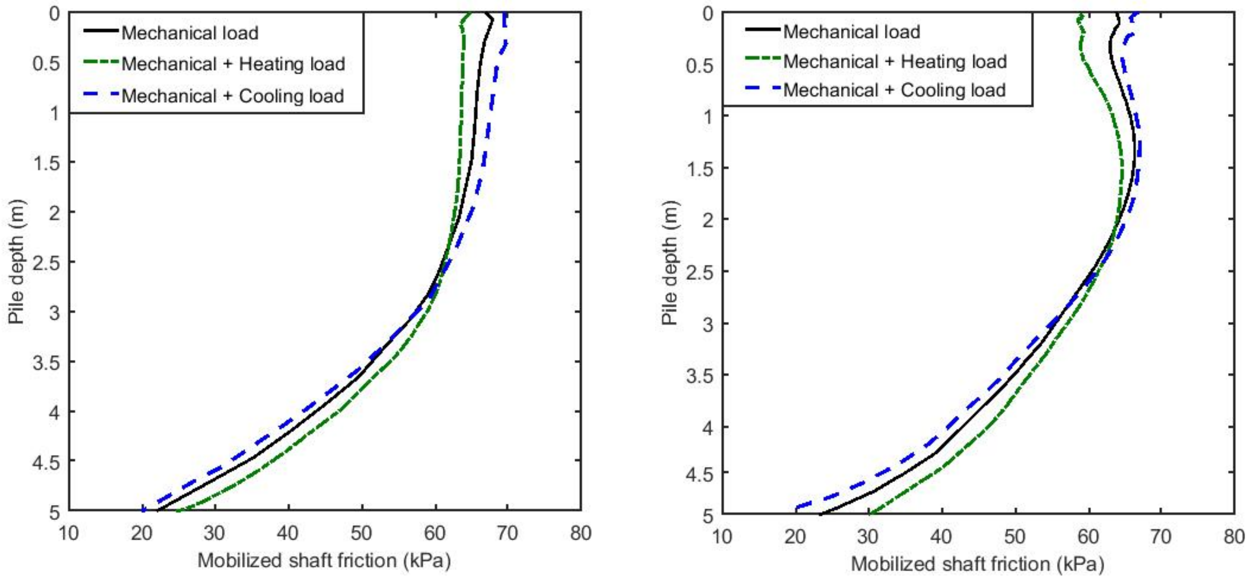

(a) Without considering the heat loss through the basement

(b) Considering heat loss through the basement

Figure 11: Mobilized shaft friction distribution along the soil-pile interface.

inlet temperature of the heat exchanger fluid was equal to -1°C, the temperature of the pile and the surrounding soil decreased. Despite the noticeable decrease, the average temperature of the soil at the pile-soil interface was equal to 3°C, which is above the freezing point. In other words, the "non freezing pile-soil interface" criterion was met using the inlet temperature of -1°C during the cooling loading stage. The temperature field at the end of the heating loading stage was shown in Fig. 12c. According to this figure, the temperature of the soil domain ranged from 8°C to 15°C.

The temperature fields of the model for Case 2 are shown in Fig. 13. The top boundary of the axisymmetric model in Case 2 was in direct contact with indoor air of the basement whose temperature assumed to be constant and equal to 20°C. Also, for the side and bottom boundaries of the model, adiabatic condition was considered. At the end of the mechanical loading stage (t = 30 days), the soil did not have enough time to absorb heat from the basement floor. Therefore, the temperature profile of the soil was equal to the initial temperature (Fig. 13a). The temperature profile at the end of cooling loading (Nov–Apr), when the inlet temperature of the heat exchanger fluid was equal to -1°C, is provided in Fig. 13b. According to this figure, the temperature of the soil surrounding the pile decreased up to 5°C although above the freezing point. In addition, the soil temperature near the basement slab increased up to 1.5°C due to the heat loss through the basement.

At the end of the heating loading stage (May–Oct), when the temperature of the heat exchanger fluid was constant and equal to 20°C, the temperature of the pile and its surrounding soil increased compared to the initial temperature (Fig. 13c). The temperature of the

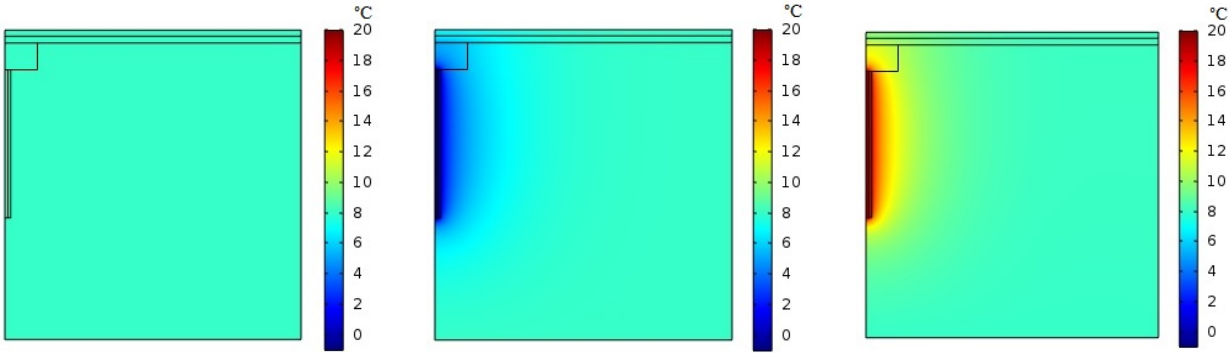

(a) Mechanical loading

(b) Cooling + mechanical loading

(c) Heating + mechanical loading

Figure 12: Temperature profiles at the end of mechanical loading; cooling and mechanical loading; and heating and mechanical loading stages for Case 1.

ground far from the effective diameter of the pile, increased up to 1.5°C especially at shallower depth of soil. This was expected to happen due to the heat dissipation through the basement of the building.

5. Conclusion

In cold regions where the heating load of the building is commonly higher than the annual cooling load, the thermal imbalance may occur in the soil due to an excessive heat extraction from the ground. In design of such systems in cold regions, the energy performance of the energy pile system is of paramount importance. The heat extraction and injection from/to the ground must be designed in such a way to avoid freezing at the pile-soil interface as well as occurring ground thermal imbalance. In addition to the energy performance of the energy pile systems, their TM behavior should be investigated as well.

Due to the lack of information regarding the effect of heat dissipation through the basement slab on the energy pile's response, a numerical study was carried out. A single geothermal friction pile of an energy foundation system that was designed for supplying the energy demand of the Stanley Pauley Engineering Building located in the Campus of the University of Manitoba, Winnipeg, Canada was considered. To this end, a 2D TM model was implemented in COMSOL Multiphysics and was validated against the field data obtained from the in-situ tests in the Lambeth College in London [14]. Based on the numerical analysis, the following conclusions can be made:

- During the cooling stage , the pile head downward displacement increased due to pile contraction. Although noticeable, the pile displacements were below the allowable pile settlement according to the National Building Code of Canada [39].
- The results verified that when the energy pile was subjected to heating and cooling loads, the thermal deformations generated additional compressive and tensile stresses during heating stage (May–Oct) and cooling stage (Nov–Apr), respectively. This necessitates further considerations in

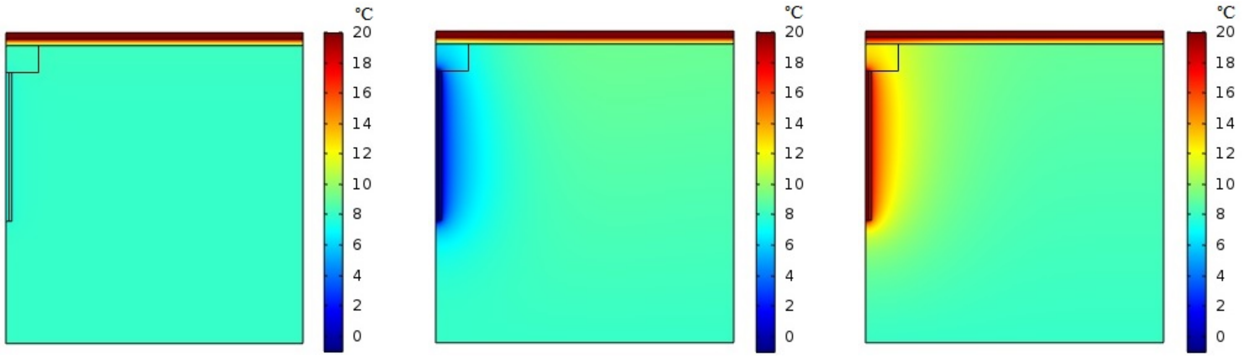

(a) Mechanical loading (b) Cooling + mechanical loading (c) Heating + mechanical loading

Figure 13: Temperature profiles at the end of mechanical loading; cooling and mechanical loading; and heating and mechanical loading stages for Case 2.

the geothechnical design and application of energy pile systems in cold regions. These considerations can be implemented in the form of increasing the factor of safety effective on the allowable load.

- The obtained results showed the importance of considering heat dissipation through the basement in evaluating the thermo-mechanical behavior of energy piles. The reason was that the heat loss through the basement worked as an additional thermal load which intensified the heating load and weakened the effects of applied cooling load on the pile.

- As the thermal loads were applied to the pile, the mobilized shaft friction along the pile-soil interface varied depending on the type of the loading stage (i.e., heating or cooling). For example, heating load caused up to a 7% decrease in shaft friction along the pile upper than the neutral point compared to shaft frictions induced during the mechanical loading stage. The same thermal load decreased the shaft friction along the pile lower than the neutral point up to 12%.

This work provided an insight into the mechanical behavior of a single pile of a energy foundation system. Result of this study in conjunction with thermal performance analysis can facilitate further application of such systems in cold regions and more specifically Canada.

6. Acknowledgment

The authors gratefully acknowledge the financial support of the NSERC CREATE SERA Program and the University of Manitoba. Also, the authors would like to acknowledge the Faculty of Engineering of the University of Manitoba for the technical support of this research.

References

[1] P. Blum, W. Campillo, G. Munch, T. Kolbel, CO2 savings of ground source heat pump systems—A regional analysis, Renewable Energy 35 (2010) 122–127.

[2] M. Kharseh, L. Altorkmany, M. Al-Khawaja, F. Hassani, Analysis of the effect of global climate change on ground source heat

pump systems in different climate categories, Renewable Energy 78 (2015) 219–225.

[3] M. Omer, Ground-source heat pump systems and applications, Renewable and Sustainable Energy Reviews 12 (2) (2008) 344–371.

[4] M. Younis, T. Bolisseti, D. Ting, Ground source heat pump systems: Current status, International Journal of Environmental Studies 67 (3) (2010) 405–415.

[5] J. U. Lee, T. Kim, S. B. Leight, Thermal performance analysis of a ground-coupled heat pump integrated with building foundation in summer, Energy and Buildings 59 (2013) 37–43.

[6] H. Brandl, Energy piles and diaphragm walls for heat transfer from and into the ground, Proc. 3rd Int. Symp. on Deep Foundations on Bored and Auger Piles, BAP III, Ghent (1998) 37–60.

[7] J. Briaud, The National Geotechnical Experimentation sites at Texas A&M University: Clay and Sand, A Summary, Geotechnical Special Publication Journal .

[8] J. Fadejev, J. Kurnitski, Y. Chen, Geothermal energy piles and boreholes design with heat pump in a whole building simulation software, Energy and Buildings 106 (2015) 23–24.

[9] L. Laloui, M. Nuth, L. Vuliet, Experimental and numerical investigations of the behaviour of a heat exchanger pile, International Journal for Numerical and Analytical Methods in Geomechanics 30 (2006) 763–781.

[10] M. Yari, N. Javani, Performance assessment of a horizontal coil geothermal heat pump, International Journal of Energy Research 31 (6) (2006) 288–299.

[11] H. Esen, Y. Inalli, M. Esen, Temperature distributions in boreholes of a vertical ground-coupled heat pump system, Renewable Energy 34 (2009) 2672–2679.

[12] N. Diao, Z. Li, Q. Fang, Heat transfer in ground heat exchangers with groundwater advection, International Journal of Thermal Science 43 (2004) 1203–1211.

[13] O. Boënnec, Piling on the Energy, Geodrilling Int 150 (2009) 25–28.

[14] P. J. Bourne-Webb, B. Amatya, K. Soga, T. Amis, C. Davidson, P. Payne, Energy pile test at Lambeth College, London: geotechncial and thermodynamic aspects of pile response to heat cycles, Géotechnique 3 (2009) 237–248.

[15] P. Bourne-Webb, B. Amatya, K. Soga, A framework for understanding energy pile behaviour, Proceedings of the Institution of Civil Engineers - Geotechnical Engineering 166 (2) (2013) 170–177.

[16] M. Andolfi, R. M. S. Maiorano, A. Mauro, N. Massarotti, On the influence of thermal cycles on the yearly performance of an energy pile, Geomechanics for Energy and the Environment 16 (2018) 32–44.

[17] B. Amatya, K. Soga, P. Bourne-Webb, T. Amis, L. Laloui, Thermo-mechanical behaviour of energy piles, Ge´otechnique 62 (6) (2012) 503–519.

[18] H. Brandl, Energy Foundations and Other Thermo-Active Ground Structures, Geotechnique 56 (2) (2006) 81–122.

[19] C. Pasten, J. Santamarina, Thermally Induced Long-Term Displacement of Thermoactive Piles, Journal of Geotechnical and Geoenvironmental Engineering 140 (5).

[20] S. Jeong, H. Lim, J. K. Lee, J. Kim, Thermally induced mechanical response of energy piles in axially loaded pile groups, Applied Thermal Engineering 71 (2014) 608–615.

[21] C. G. Olgun, T. Y. Ozudogru, S. L. Abdelaziz, A. Senol, Long-term performance of heat exchanger piles, Acta Geotechnica 10 (2015) 553—-569.

[22] M. Saaly, P. Maghoul, M. Kavgic, D. Polyzois, Performance Analysis of a proposed geothermal pile system for heating and cooling energy demand for a building in cold regions, Sustainable Cities and Societies 45 (2019) 669–682.

[23] H. Liu, P. Maghoul, H. Holländer, Sensitivity analysis and optimum design of a hydronic snow melting system during snowfall, Physics and Chemistry of the Earth, Parts A/B/C doi: 10.1016/j.pce.2019.01.009.

[24] C. Dacquaya, H. Holländer, M. Kavgic, P. Maghoul, H. Liu, H. Fujii, Evaluation of an integrated sewage pipe with ground heat exchanger for long-term efficiency estimation, Geothermics 86 (2020) 101796, doi:10.1016/j.geothermics.2019.101796.

[25] A. Hepbasli, O. Akdemir, E. Hancioglu, Experimental study of a closed loop vertical ground source heat pump system, Energy Conversion and Management 44 (4) (2003) 527–548.

[26] H. Liu, P. Maghoul, A. Bahari, M. Kavgic, Feasibility Study of Snow Melting System Using Geothermal Energy Heat Pumps in

Canada, Renewable Energy 136.

[27] A. Fergusen, A. D. Woodbury, Subsurface heat flow in an urban environment, Journal of Geophysical Research 109 (2004) 1–9.

[28] M. Saaly, K. Bobko, P. Maghoul, M. Kavgic, H. Holländer, Energy performance of below-grade envelope of an institutional building in cold regions, Journal of Building Engineering 27.

[29] M. Andolfi, R. M. S. Maiorano, A. Mauro, N. Massarotti, Experimental set-up and thermo hydro mechanical model for an energy pile, Proceedings of a conference on computational methods for thermal problems Atlanta, USA, Georgia Tech.

[30] C. Cekerevac, L. Laloui, Experimental study of thermal effects on the mechanical behavior of a clay, International Journal of Numerical Methods in Geomechanics 28 (3) (2004) 209–228.

[31] Environment and Climate Change Canada, Winnipeg Historical Temperature, URL `https://winnipeg.weatherstats.ca/`, 2019.

[32] A. Al-Janabi, M. Kavgic, A. Mohammadzadeh, A. Azzouz, Comparison of EnergyPlus and IES to model a complex university building using three scenarios: Free-floating, ideal air load system, and detailed, Journal of Building Engineering 22 (2019) 262–280.

[33] D. Essex, K. Joe, H. Arvinder, L. Russell, F. Danial, G. Kaeryn, R. John, Project Manual. Volume I of II Stanley Pauley Engineering Building 97 Dafoe Road (Vol. I). University of Manitoba., 2017.

[34] A. E. Delsante, A. N. Stokes, P. J. Walsh, Application of Fourier Transforms to Periodic Heat Flow Into the Ground Under a Building, Internationa! Journal of Heat and Mass Transfer (26) (1982) 121–132.

[35] M. Karti, D. E. Claridge, J. Kreider, ITPE technique applications to time-varying three-dimensional groundcoupling problems, ournal of Heat Transfer (ASME) 112 (1990) 849–852.

[36] A. H. Lachenbruch, Three-Dimensional Heat Conduction in Permafrost Beneath Heated Buildings, Geological Survey Bulletin 1052-B, U.S. Government Printing Office, Washington, DC. .

[37] M. G. Davies, Heat loss from a solid ground floor, Building and Environment 28 (3) (1993) 347–359.

[38] D. Chen, Heat Loss via Concrete Slab Floors in Australian Houses, Procedia Engineering 205 (2017) 108–115, doi: 10.1016/j.proeng.2017.09.941.

[39] The National Building Code of Canada 2015 (NBC), National Research Council Canada .